

An Optimization Method to Determine Optimum Carbonization Temperature of Banana Stems Based Activated Carbon for Supercapacitors

by Erman Taer

Submission date: 19-Feb-2020 03:13PM (UTC+0700)

Submission ID: 1260073215

File name: Taer_2019_IOP_Conf._Ser.__Mater._Sci._Eng._599_012030.pdf (1.07M)

Word count: 4425

Character count: 23176

PAPER • OPEN ACCESS

An Optimization Method to Determine Optimum Carbonization Temperature of Banana Stems Based Activated Carbon for Supercapacitors

5

To cite this article: Erman Taer *et al* 2019 *IOP Conf. Ser.: Mater. Sci. Eng.* **599** 012030

View the [article online](#) for updates and enhancements.

**IOP | ebooks™**

Bringing you innovative digital publishing with leading voices
to create your essential collection of books in STEM research.

Start exploring the collection - download the first chapter of
every title for free.

An Optimization Method to Determine Optimum Carbonization Temperature of Banana Stems Based Activated Carbon for Supercapacitors

Erman Taer^{1,*}, Agrandi Purnama¹, Apriwandi¹, Agustino¹, Rika Taslim² and Widya Sinta Mustika^{1,3}

¹Department of Physics, University of Riau, 28293 Simpang Baru, Riau, Indonesia

²Departement of Industrial Engineering, State Islamic University of Sultan Syarif Kasim, 28293 Simpang Baru, Riau, Indonesia

³Department of Physics, Institute Technology of Bandung, Bandung, West Java, Indonesia

*E-mail: erman_taer@yahoo.com

Abstract. The optimization of carbonization temperature was obtained by experimental design, assisted by using a 3rd-order polynomial equation, for use in supercapacitor application. Activated carbon monoliths are produced based on the carbonization temperatures of 500 °C, 550 °C, 600 °C and 650 °C. The monolithic activated carbon samples were characterized based on their physical properties, including density, degree of crystallinity and surface morphology, and their electrochemical properties, including specific capacitance, energy and power. The optimum conditions, which yielded a minimum electrode density and steak height as well as a maximum combination of energy and power, were found to be at a temperature of approximately 550 °C. In addition, the exact minimum and maximum carbonization temperatures that correlated with density, steak height and a combination of energy and power were found by a simulated mathematical model to be 543 °C, 544 °C, and 553 °C, respectively. The surface morphology was analyzed and was used as supporting data. In conclusion, by experimental and mathematical simulation, the optimum carbonization condition was obtained more accurately.

1. Introduction

Supercapacitors have attracted the interest of many researchers in recent years because they have several advantages, such as a high energy density, maximum power, long life cycle and short charge-discharge time. Supercapacitors are composed of electrodes, electrolytes, separators and current collectors. Studies on supercapacitors have been widely undertaken, with one of the main focuses being modifications to the electrodes. Electrodes can be produced from biomass materials such as rubber wood [1], oil palm empty fruit bunches [2], banana peels [3], rice husks [4] and tea leaves [5]. Biomass materials are selected as the raw materials for the manufacture of supercapacitor electrodes for several reasons, such as ease of production at low carbonization temperature, easy activation, low production cost and abundant availability [6]. Pyrolysis, otherwise known as carbonization, is a common method used in the production of supercapacitor electrodes from biomass materials. Several factors that affect pyrolysis are the type of inert gas, the gas flow rate and the maximum temperature of carbonization, which in turn affects the kinetic energy of the inert gas. A high temperature can lead



Content from this work may be used under the terms of the Creative Commons Attribution 3.0 licence. Any further distribution of this work must maintain attribution to the author(s) and the title of the work, journal citation and DOI.

Published under licence by IOP Publishing Ltd

to high collision energies between the inert gas molecules and the atoms of the biomass material, resulting in the breaking of bonds between carbon and non-carbon atoms so that organic carbon content from biomass can be converted into porous carbon materials. The optimum carbonization temperatures produce a maximum percentage of carbon [7, 8]. The percentage of carbon on the electrode affects the number of ion pairs and electrons formed in the supercapacitor cell. The electron-ion pair occurs at the interface of the electrode and the electrolyte. The number of charge pairs formed determines the capacitive behavior of the supercapacitor cell. A high carbon content also increases the probability of forming charge pairs. The optimum transformation of biomass materials into carbon materials occurs at the optimum temperature of carbonization, with each type of biomass having a unique optimum carbonization temperature. This condition needs to be considered in choosing the temperature of carbonization. Ma, et. al. (2015) [9] produced supercapacitor cell electrodes by carbonizing potato waste residue (PWR) at a temperature range of 600-900 °C and obtained a specific capacitance of 255 F.g⁻¹ at 700 °C. The production of electrodes from ramie in a carbonization temperature range of 400-750 °C resulted in a maximum capacitance of 287 F.g⁻¹ at a carbonization temperature of 650 °C [10]. Meanwhile, carbon electrodes from algae produce a specific capacitance of 234 F.g⁻¹ at a carbonization temperature of 700 °C, wherein carbonization is observed at a temperature range of 700-900 °C [11]. The objective of this study was to review the maximum carbonization temperature for the production of supercapacitor cell electrodes from banana stem biomass residues. This study was conducted by combining experimental methods and mathematical modeling with polynomial equations. A combination of experimental methods and mathematical modeling to obtain the optimum activation temperature in the production of activated carbon from luscious char [12], coconut husk [13] and palm shell [14] have been performed using quadratic equations based on central composite design (CCD). Faramarzi (2015) [15] and Musabbikhah (2017) [16] optimized the production process of activated carbon from pistachio shell and rice husk through a mathematical model approach through Taguchi's experimental design. Taguchi's experimental design requires many variables, such as particle size, carbonization temperature, heating rate, holding time, and the N₂ gas flow rate in determining the optimum conditions for the activation of carbon. This approach may get more accurate results but may take a relatively longer time. This study will carry out an optimization of the carbonization temperature in the production process of activated carbon monoliths from banana stems with a mathematical approach using a 3rd order polynomial equation. The mathematical equation used is simpler than the methods previously reported, whereas the more extensive discussion involves the density, stack height, energy and power of a supercapacitor cell.

2. Experimental Method

2.1. The Electrode preparation and cell fabrication

Activated carbon monolith electrodes were produced from banana stems by previously reported methods [17]. Banana stems were first cut into square shapes ± 2 cm. Furthermore, the banana stems were dried and carbonized at 250 °C for 2.5 hours to obtain a carbonized banana stem that had adhesive properties. The next step involved smoothing using ball milling for 20 hours and sieving to obtain a particle size of 38-53 µm. The powder sample was then activated with 0.4 M KOH. The activated powder sample was molded into pellets to produce Green Monolith Banana Stem (GMBS) electrodes [17] that had a diameter of ± 2 cm and a thickness of ± 2 mm. The GMBS pellet was modified into a carbon pellet electrode through a stage of integrated carbonization and physical activation using a furnace [18]. This stage began with carbonization carried out under N₂ gas at a temperature that varied from room temperature to a maximum temperature, followed by physical activation using CO₂ [19] at a temperature of 850 °C with a 2-hour holding time. This process produced an activated carbon monolith (ACM). The carbonization temperatures were 500 °C, 550 °C, 600 °C and 650 °C; each ACM sample was thus labeled ACM500, ACM550, ACM600 and ACM650. All the ACM pellets were polished to the desired thickness and were washed with neutral (pH 7) water. The supercapacitor cells were arranged in a sandwich that comprised the insulator body supercapacitor, current collector, electrode, electrolyte and separator, as we have reported in previous research [20][21].

2.2. Physical Characteristics

The physical properties of the ACM analyzed include density, structure, surface morphology and chemical composition. The density was calculated from the mass, diameter and thickness of the electrodes. The ACM structure was analyzed using X-ray Diffraction (XRD). XRD measurements were performed using a Philip X-Pert Pro PW 3060/10 instrument with a K- α ray source at a wavelength of 1.5418 Å and diffraction angles of $2\theta = 10$ -100 degrees. The surface morphology was examined using scanning electron microscopy (SEM) with a SUPRA instrument, S-3400N series. The composition of ACM contents was determined by energy dispersive X-ray (EDX) spectroscopy.

2.3. Electrochemical Characteristics

The electrochemical properties of the supercapacitor cells were analyzed using a Physics CV UR Rad-Er 5841 instrument and were calibrated with Solartron 1280 devices. Electrochemical measurements were carried out at a rate of 1 mV.s⁻¹ and a potential of 0 s / d of 500 mV controlled using the Cyclic Voltammetry software CVv6. The specific capacitance, energy and power were calculated by using the standard formula [22] [23].

$$C_{sp} = \frac{I_c - I_d}{sm} \quad E = \frac{1}{2} C_{sp} \Delta V^2 \quad P = \frac{E}{\Delta t} \quad (1)$$

3. Result and Discussion

3.1. Physical Properties Analysis

The ACM density data were obtained from the calculation of the mass, diameter and mean thickness by using the standard formula ($\rho = m / V$). The density of each ACM was reported after the integrated carbonization-activation process and is shown in Figure 1 a. The densities of ACM500, ACM550, ACM600 and ACM650 were 0.808 g cm⁻³, 0.733 g cm⁻³, 0.790 g cm⁻³ and 0.813 g cm⁻³, respectively. ACM550 showed a lower density than did ACM500. The increase in the carbonization temperature for ACM550 led to a greater loss of materials other than carbon, such as moisture content, compared to ACM500, resulting in a significant decrease in mass. The ACM550, ACM600 and ACM650 samples showed a linear trend of increasing density values; an increase in carbonization temperature resulted in an increase in density. In this case, the increase in carbonization temperature resulted in a smaller decrease in mass than a decrease in volume. The mass loss during the carbonization process led to the rearrangement of carbon atoms to form stronger bonds, causing dimension shrinkage.

The density as a function of carbonization temperature was fit using the 3rd-order polynomial shown in Figure 1a. The 3rd-order polynomial equation indicated a minimum density of 0.7329 g cm⁻³ at a carbonization temperature of 543 °C. The polynomial approach supported the experimental results to obtain a more appropriate minimum density. Figures 1b and 1c show micrograph SEM data for the ACM550 and ACM600 samples. These two samples showed differences in the arrangement of carbon microparticles; ACM550 showed more inter-particle pores than the ACM600 sample. The ACM600 sample showed inter-particle pores covered by smaller particles with irregular shapes as well as by fibers. This difference indicated that the increase in carbonization temperature caused the particles to break into finer particles, resulting in the release of fibers. This SEM data supported the relationship between density and carbonization temperature, as shown in Figure 1a, wherein the minimum density occurred at approximately of 550 °C

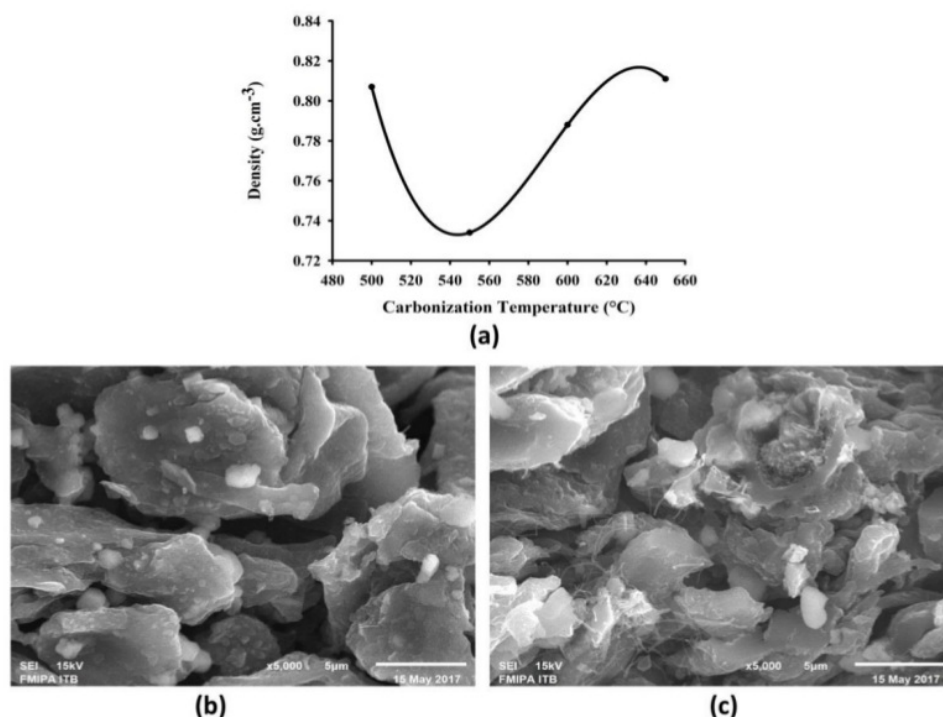


Figure 1. a) Density modeling curve; b) micrograph SEM for ACM550; c) micrograph SEM for ACM600.

The X-Ray diffraction curves for all of the ACM samples is shown in Figure 2. This figure, which plots the X-ray intensity as a function of the diffraction angle, showed no significant difference. In general, Figure 2a shows that the samples of ACM produced two broadening peaks and the same sharp peaks. The broadening peak appeared at a diffraction angle 2θ of $24.827^\circ - 25.333^\circ$ and $44.542^\circ - 46.505^\circ$ for reflection planes of 002 and 100, respectively [24]. The presence of broadening peaks in the diffractogram showed that the ACM sample had an amorphous carbon structure [25]. In addition, the sharp peaks, due to the presence of impurities other than carbon material, had a crystalline structure. This condition was caused by the heating process in the modification of carbon from biomass, which produced other materials such as silica [2], potassium and magnesium. The chemical activation process also produced impurities in the sample caused by the imperfect washing process.

The variations of carbonization temperature used in the production of ACM resulted in microcrystallite dimensions. The microcrystallite dimension, such as stack height (L_c), was calculated using the Debye-Scherrer equation [26 - 28] and $L_c = 0.89 \lambda / \beta \cos \theta_{(002)}$, where λ is the wavelength (Å), β is the bandwidth (degrees), $\theta_{(100)}$ is the diffraction angle in the hkl plane 100 (degrees) and $\theta_{(002)}$ is the diffraction angle in the hkl plane 002 (degrees) [29]. Differences in the temperature of carbonization used also resulted different values of microcrystallite dimensions.

The relationship between the L_c and the carbonization temperature was expressed in the 3rd-order polynomial shown in Figure 2b. The smallest L_c was obtained at a carbonization temperature slightly lower than 550°C . The minimum L_c was obtained by using the inserted 3rd-order polynomial in Figure 2b; the minimum L_c obtained was 11,5617 (Å) at a carbonization temperature of 544°C . The relationship between electrode density and L_c can be observed in Figures 1a and 2b, where the

minimum density occurred when L_c was also the minimum. In other words, the minimal density and L_c minimum occurred at almost the same carbonization temperature. These results indicate that density changes in the biomass-based carbon electrode, as a function of the carbonization temperature, were influenced by the arrangement of carbon particles in the height direction, or L_c .

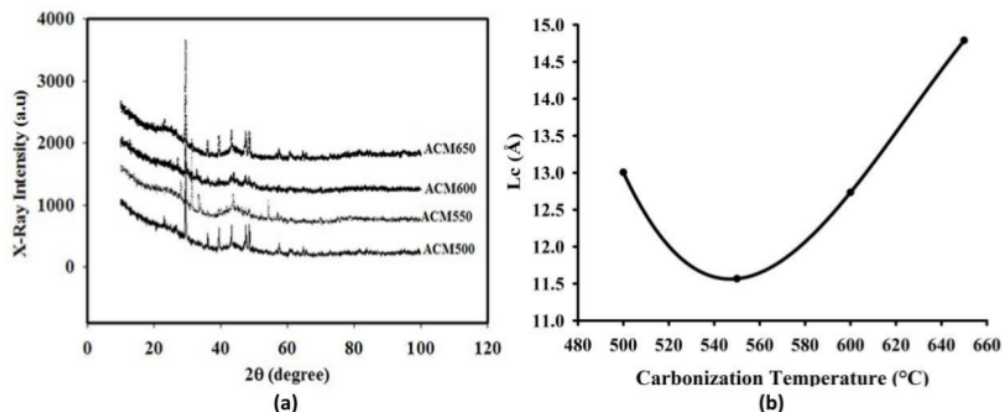


Figure 2. a) Diffractogram curves for ACM; b) polynomial curve of L_c and carbonization temperature.

3.2 Electrochemical Properties Analysis

The cyclic voltammetry (CV) measurement data for the ACM samples are shown in Figure 3a. The current density was plotted as a function of voltage, at a scan rate of 1 mV.s^{-1} . All the samples showed an almost identical curve. The current charging process for each ACM sample started at a potential of 0.0 V, while the current discharge process began at a potential of 0.5 V [30]. The charging and discharging current rates indicate the shape and pore size of the carbon electrode. The difference in the rate of current at a potential slightly larger than 0.0 V indicates the difference in the number of pores on the carbon electrode. The process of ion diffusion from the electrolyte into the pores that exist on the surface of the carbon electrode affects the number of electron pairs formed on the carbon electrode, thereby increasing the current and increasing the specific capacitance of the supercapacitor cell. Figure 3a also shows the area between different charge and discharge currents, at a potential of 0.25 V. ACM500, ACM550 and ACM600 produced a curve with a minimum increase after the maximum current charge from a potential that was slightly lower than 0.0 V to a maximum potential window of 0.5 V. The presence of an increase in slope indicated the presence of a dominant amount of micropores in the electrode samples. ACM550 produced a wider gap between the charge and discharge curves than that of ACM500, which corresponded to an increase in the number of micropores carbon electrode. The increase in carbonization temperature for ACM600 produced a lower curve than that of ACM550. An increase in carbonization temperature of up to 600 °C reduced the number of micropores on the carbon electrode [7]. However, the ACM650 produced a flatter curve shape after the maximum current charge at a potential of 0.0 V. The flatter curve indicated that the charging process, with ions moving into the micropore, had finished when the potential was larger than 0.2 V.

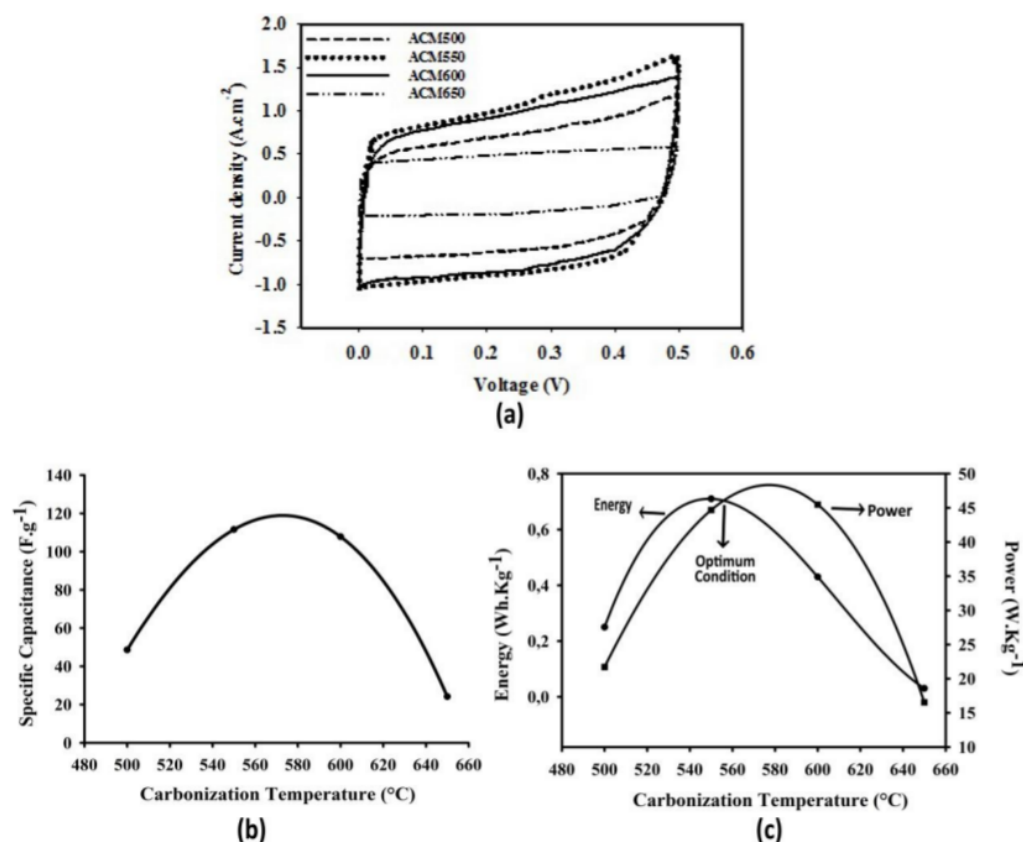


Figure 3. a) CV curve for ACM; b) polynomial curve of C_{sp} and carbonization temperature; c) polynomial curves of energy and power with carbonization temperature.

The CV measurement resulted in the charging current (I_c) and discharging current (I_d); by using the same formulas [2, 22], one can calculate the specific capacitance (C_{sp}) of the electrode as well as the specific energy (E) and power (P) of the supercapacitor cell. The C_{sp} initially increased with increasing carbonization temperature. At a carbonization temperature of 500 °C, the C_{sp} was 48.58 F g⁻¹; when the carbonization temperature was increased to 550 °C, the C_{sp} was as high as 111.56 F g⁻¹. However, as temperatures continued to increase to 600 °C and 650 °C, the C_{sp} decreased as the carbonization temperature increased; the C_{sp} values were 107.80 F g⁻¹ and 24.15 F g⁻¹, respectively. It can be concluded that the optimum carbonization temperature was between 550 °C and 600 °C. The optimum carbonization temperature, corresponding to the optimum C_{sp}, can be calculated using polynomial equation fitting. Figure 5 was obtained by fitting the C_{sp}, as a function of carbonization temperature, to a 3rd-order polynomial. The fit showed that the best carbonization temperature for the ACMs from banana stems was in the range 550–600 °C, exactly 572 °C, with an optimum C_{sp} as high as 119 F g⁻¹. In addition, the resulting capacitive electrode is almost the same as the other capacitive electrode with a different biomass such as durian shell as high as 88.39 F g⁻¹ [31], banana stem 170 F g⁻¹ [32] and corn stalk as high as 140 F g⁻¹ [33].

The energy and power obtained from the experimental data were also fit using a 3rd-order polynomial. These data are shown in Figures 3c. The maximum energy of 0.7101 Wh kg⁻¹ was obtained at a carbonization temperature of 548 °C, while a maximum power of 48.3531 W kg⁻¹ was obtained at a carbonization temperature of 577 °C. These results indicate that there was little

difference in optimum carbonization temperature conditions for the Csp, energy and power produced by the supercapacitor cells. The optimum condition of a supercapacitor cell is an optimum combination of energy and power. Figure 3c shows that the energy and power curves intersected at a certain point; this intersection point indicated the optimum condition of energy and power. This intersection point appeared at a carbonization temperature of 553 °C. This point is indicated by arrows in Figure 3c. This temperature was selected as the optimum carbonization temperature for the production of supercapacitor electrodes from banana stem waste material. This optimum carbonization temperature is almost equal to the optimum temperature of carbonization in other material samples, such as rubber wood sawdust [20] and bamboo waste [34].

Table 1. Coefficient parameters of the 3rd-order polynomial equation

Parameters	Coefficients			
	y_0	a	b	c
Density (g cm ⁻³)	43.2820	-0.2188	0.0004	-2,1067E-007
Steak height (Å)	549.4660	-2.6532	0.0043	-2.2947E-006
Csp (F g ⁻¹)	-1358.9200	-0.5927	0.0156	-1.7533E-005
Energy (Wh kg ⁻¹)	-181.4500	0.9127	-0.0015	8.2667E-007
Power (W kg ⁻¹)	230.2600	-3.9788	0.0122	-1.0053E-005

The mathematical equation used in analyzing the experimental results, to determine the optimum value of density, steak height, Csp, energy and power, is

$$f = y_0 + ax + bx^2 + cx^3 \quad (2)$$

which is known as a 3rd-order polynomial equation. This 3rd-order polynomial is a cubic polynomial with one variable. The mathematical equations obtained had a correlation coefficient (R) equal to 1.00, which means that the equations used had a perfect correlation. Coefficients y_0 , a , b and c are real coefficients obtained using Ms.excel, if all coefficients are real numbers then 3rd-order polynomial solutions have more than one real root or critical point, but in the data shown in Figure 3a and 3b only one critical point appears due to the limited of data. This critical point signify the optimum conditions of each parameters being modeled. This simple modeling helps researchers to determining optimum conditions faster and easier without the use of complicated software. The coefficients of the 3rd-order polynomial equations (such as y_0 , a , b and c) for density, steak height, Csp, energy and power can be seen in Table 1. The density and steak height modeling showed curves with a minimum value, whereas the modeling data for Csp, energy and power showed curves with a maximum value.

In general, the results of the analysis of the physical and electrochemical properties as a function of the carbonization temperature of the carbon electrode supercapacitor showed a connection among density, surface morphology, steak height and the combination of energy and power. The minimum density and minimum L_c occurred at nearly equal carbonization temperatures, and these conditions also led to an optimum combination of energy and power. It can be concluded that the experimental approach and the associated 3rd-order polynomial equation have been successfully used to obtain the optimum temperature conditions for the combination of energy and power. Finally, the experimental approach and the 3rd-order polynomial equation shown in this paper can be considered as one way of determining the best temperature variables in the process of preparing supercapacitor electrodes, such as the temperatures of carbonization and activation.

4. Conclusion

The optimum physical and electrochemical properties of carbon electrodes have been successfully found experimentally, assisted by mathematical modeling using a 3rd-order polynomial equation. Varying the carbonization temperature in the preparation process resulted in different physical and electrochemical properties. The experimental data were fitted by using a 3rd-order polynomial

equation to find the optimum conditions. The information in the mathematical models was analyzed, and the corrected optimum condition was found, for the experimental data. Finally, the mathematical modeling approach that has been shown can determine the optimum conditions of carbonization temperature more accurately.

5. References

- [1] Taer E, Taslim R and Deraman M 2016 *AIP Conf. Proc.* **1712** 050011-1
- [2] Farma R, Deraman M, Awitdrus A, Talib I A, Taer E, Basri N H, Manjunatha J G, Ishak M M, Dollah B N M and Hashmi S A 2013 *Bioresource Technol.*, **132** 254
- [3] Taer E, Taslim R, Aini Z, Hartati S D and Mustika W S 2017 *AIP Conf. Proc.* **1801** 040004
- [4] Teo E Y L, Muniandy L Ng E, Adam F, Mohamed A B, Jose R and Chong K F 2016 *Electrochim. Acta* **192** 110
- [5] Peng C, Yan X, Wang R, Lang J, Ou Y and Xue O 2013 *Electrochim. Acta* **87** 401
- [6] Abioye D M and Ani F N 2015 *Renewable and Sustainable Energy Reviews* **52** 1282
- [7] Daud W M A W, Ali W S W and Sulaiman M Z 2000 *Carbon* **38** 1925
- [8] Li W, Yang K, Peng J, Zhang L, Guo S and Xia H 2008 *Industrial crops and products* **28** 190
- [9] Ma G, Yang Q, Sun K, Peng H, Ran F, Zhao X and Lei Z 2015 *Bioresource Technol.* **197** 137
- [10] Du X, Zhao W, Wang Y, Wang C, Chen M, Qi T, Hua C and Ma M 2013 *Bioresource Technol.* **149** 31
- [11] Tian Z, Xiang M, Zhou J, Hu L and Cai J 2016 *Direct Carbonization and Excellent Electrochemical Properties* **211** 225
- [12] Azargohar R and Dalai A K 2005 *Microporous and Mesoporous Mater* **85** 219
- [13] Tan I A W, Ahmad A L and Hameed B H 2008 *Chemical Engineering Journal* **137** 462
- [14] Arami-Niya A, Daud W M A W, Mjalli F S, Shafeeyan M S and Abnisa F 2012 *Chemical engineering research and design*, **90** 776
- [15] Faramarzi A H, Kaghazchi T, Ebrahim H A and Ebrahimi A A 2015 *J. Anal. Appl. Pyrolysis*
- [16] Musabbikah, Saptoadi H, Subarmono and Wibisono M A 2017 *Int. J. Renew. Energy Research* **7** 1219
- [17] Farma R, Deraman M, Omar R, Awitdrus, Ishak M M, Taer E, and Talib I A 2011 *AIP Conf. Proc.* **1415** 180.
- [18] Taer E, Apriwandi, Yusriwandi, Mustika W S, Zulkifli, Taslim R, Sugianto, Kurniasih B, Agustino and Dewi P 2018 *AIP Conf. Proc.* **1927** 030036-1
- [19] Deraman M, Ishak M M, Farma R, Awitdrus, Taer E, Talib I A, Omar R 2011 *AIP Conf. Proc.* **1415** 175
- [20] Taer E, Deraman M, Taslim R and Iwantono 2013 *AIP Conf. Proc.* **1554** 33
- [21] Taer E, Sugianto, Sumantre M A, Taslim R, Iwantono, Dahlan D, Deraman M 2014 *Adv. Mater. Res.* **896** 66
- [22] Li L, Liu E, Li J, Yang Y, Shen H, Huang Z, Xiang X and Li W 2010 *J. Power Sources* **195** 1516
- [23] Zhao Y-Q, Lu M, Tao P-Y, Zhang Y-J, Gong X-T, Zhang G-Q, Li H-L, Yang Z 2017 *J. Power Sources* **307** 391
- [24] Nabais J M V, Teixeira J G and Almeida I 2011 *Bioresource Technol.* **102** 2781
- [25] Deraman M, Omar R, Zakaria S, Mustapa I R and Talib M 2002 *J. Mater. Science* **37** 3329
- [26] Cullity B D 2001 *Elements of X-Ray Diffraction*, Ed. 3, Amazon Prentice Hall
- [27] Awitdrus, Deraman M, Talib I A, Omar R, Jumali M H, Taer E and Saman M H 2010 *Sains Malaysiana* **39** 83
- [28] Nabais J M V, Teixeira J G and Almeida I 2010 *Bioresource Technol.* **102** 2781
- [29] Carrott P J M, Nabais J M V, Carrott M M L R and Pajares J A 2001 *Carbon* **39** 1543
- [30] Inagaki M, Konno H and Tanaike O 2010 *J. Power Sources* **195** 7880
- [31] Taer E, Dewi P, Sugianto, Syech R, Taslim R, Salomo, Susanti Y, Purnama A, Apriwandi, Agustino and Setiadi R N 2018 *AIP Conf. Proc.*, **1927** 030026-1

- [32] Taer E, Taslim R, Mustika W S, Kumiasih B, Agustino, Afrianda A and Apriwandi 2018 *Int. J. Electrochem, Sci*, **13** 8428
- [33] Yu K, Zhu H, Qi H and Liang C 2018 *Diamond & Related Mater.* **88** 18.
- [34] Zhang Y-J, Xing Z-J, Duan Z-K, Li M and Wang Y 2014 *Applied Surface Science* **315** 279

2

Acknowledgements

The author would like to thank the DRPM Kemenristek-Dikti through the second year Project of DUPT with the title “Potential of Urban Solid Waste Utilization as a Supercapacitor Electrode” with contract number: 360/UN.19.5.1.3/PP/2018. The author also thanks the SEM FMIPA ITB Laboratory, which has assisted in obtaining the SEM and EDX data.

An Optimization Method to Determine Optimum Carbonization Temperature of Banana Stems Based Activated Carbon for Supercapacitors

ORIGINALITY REPORT

19%

SIMILARITY INDEX

10%

INTERNET SOURCES

16%

PUBLICATIONS

%

STUDENT PAPERS

PRIMARY SOURCES

1

dspace.vutbr.cz

Internet Source

3%

2

E Taer, R Radiawan, R Taslim, Awitdrus, A Apriwandi, Krisman, Minarni, A Agustino, R Farma, R N Setiadi. "The effect of microwave irradiation in activated carbon processing from sago waste to physical and electrochemical properties of electrode supercapacitor cells", Journal of Physics: Conference Series, 2018

Publication

2%

3

www.science.gov

Internet Source

2%

4

E Taer, A Apriwandi, Krisman, Minarni, R Taslim, A Agustino, A Afrianda. "The physical and electrochemical properties of activated carbon electrode made from pandanus tectorius", Journal of Physics: Conference Series, 2018

Publication

1%

5	elar.usfeu.ru Internet Source	1 %
6	E. Taer, Y. Susanti, Awitdrus, Sugianto, R. Taslim, R. N. Setiadi, S. Bahri, Agustino, P. Dewi, B. Kurniasih. "The effect of CO2 activation temperature on the physical and electrochemical properties of activated carbon monolith from banana stem waste", AIP Publishing, 2018 Publication	1 %
7	www.mdpi.com Internet Source	1 %
8	E. Taer, M. Deraman, I.A. Talib, S.A. Hashmi, A.A. Umar. "Growth of platinum nanoparticles on stainless steel 316L current collectors to improve carbon-based supercapacitor performance", Electrochimica Acta, 2011 Publication	<1 %
9	Sultan Ahmed, Ahsan Ahmed, M Rafat. "Nitrogen doped activated carbon from pea skin for high performance supercapacitor", Materials Research Express, 2018 Publication	<1 %
10	Laura Guardia, Loreto Suárez, Nausika Querejeta, Roberto Rodríguez Madrera, Belén Suárez, Teresa A. Centeno. "Apple Waste: A	<1 %

Sustainable Source of Carbon Materials and Valuable Compounds", ACS Sustainable Chemistry & Engineering, 2019

Publication

11

Ahmad Taghizadeh-Alisaraei, Hossein Alizadeh Assar, Barat Ghobadian, Ali Motevali. "Potential of biofuel production from pistachio waste in Iran", Renewable and Sustainable Energy Reviews, 2017

Publication

<1 %

12

E Taer, A Afrianda, R Taslim, Krisman, Minarni, A Agustino, A Apriwandi, U Malik. "The physical and electrochemical properties of activated carbon electrode made from Terminalia Catappa leaf (TCL) for supercapacitor cell application", Journal of Physics: Conference Series, 2018

Publication

<1 %

13

A.K. Choudhary, A. Dwivedi, A. Bahadur, T.P. Yadav, S.B. Rai. "Enhanced upconversion emission and temperature sensor sensitivity in presence of Bi ³⁺ ions in Er ³⁺ /Yb ³⁺ co-doped MgAl ₂ O ₄ phosphor", Ceramics International, 2018

Publication

<1 %

14

Erman Taer, Rika Taslim. "Brief review: Preparation techniques of biomass based activated carbon monolith electrode for

<1 %

supercapacitor applications", AIP Publishing, 2018

Publication

15

www.ukm.edu.my

Internet Source

<1 %

16

Donggue Lee, Yoon-Gyo Cho, Hyun-Kon Song, Sang-Jin Chun, Sang-Bum Park, Don-Ha Choi, Sun-Young Lee, JongTae Yoo, Sang-Young Lee. "Coffee-Driven Green Activation of Cellulose and Its Use for All-Paper Flexible Supercapacitors", ACS Applied Materials & Interfaces, 2017

Publication

<1 %

17

E Taer, W S Mustika, Agustino, Fajarini, N Hidayu, R Taslim. "The Flexible Carbon Activated Electrodes made from Coconut Shell Waste for Supercapacitor Application", IOP Conference Series: Earth and Environmental Science, 2017

Publication

<1 %

18

repository.ubaya.ac.id

Internet Source

<1 %

19

Leizhi Zheng, Shuang Wang, Yanfang Yang, Xiaoqi Fu, Tingshun Jiang, Juan Yang. "Ammonium Nitrate-Assisted Synthesis of Nitrogen/Sulfur-Codoped Hierarchically Porous Carbons Derived from Ginkgo Leaf for

<1 %

20

P. Staciwa, U. Narkiewicz, D. Sibera, D. Moszyński, R. J. Wróbel, R. D. Cormia. "Carbon Spheres as CO₂ Sorbents", Applied Sciences, 2019

Publication

21

Jedsada Sodtipinta, Taweechai Amornsakchai, Pasit Pakawatpanurut. "Nanoporous carbon derived from agro-waste pineapple leaves for supercapacitor electrode", Advances in Natural Sciences: Nanoscience and Nanotechnology, 2017

Publication

22

R. Farma, M. Deraman, A. Awitdrus, I.A. Talib, E. Taer, N.H. Basri, J.G. Manjunatha, M.M. Ishak, B.N.M. Dollah, S.A. Hashmi. "Preparation of highly porous binderless activated carbon electrodes from fibres of oil palm empty fruit bunches for application in supercapacitors", Bioresource Technology, 2013

Publication

23

Arvinder Singh, Amreesh Chandra. "Graphite oxide/polypyrrole composite electrodes for achieving high energy density supercapacitors", Journal of Applied Electrochemistry, 2013

Publication

<1 %

<1 %

<1 %

<1 %

24

Xiao Liu, Huanlei Wang, Yongpeng Cui, Xiaonan Xu, Hao Zhang, Gaofer Lu, Jing Shi, Wei Liu, Shougang Chen, Xin Wang. "High-energy sodium-ion capacitor assembled by hierarchical porous carbon electrodes derived from Enteromorpha", Journal of Materials Science, 2018

Publication

<1 %

25

Huaihao Zhang, Yuanyuan Jiang, Yongfeng Hu, Aimee MacLennan, Hui Wang, Chengyin Wang. "Effect of Pyrite in Precursor on Capacitance Behavior of Prepared Activated Carbon", Industrial & Engineering Chemistry Research, 2014

Publication

<1 %

26

Xinlong Yan, Qingxun Hu, Xinmei Liu, Zifeng Yan. "Comparative studies of three kinds of activated carbon reactivated by KOH", Asia-Pacific Journal of Chemical Engineering, 2012

Publication

<1 %

27

B N M Dolah, M A R Othman, M Deraman, N H Basri, R Farma, I A Talib, M M Ishak. "Supercapacitor Electrodes from Activated Carbon Monoliths and Carbon Nanotubes", Journal of Physics: Conference Series, 2013

Publication

<1 %

28

nanoscalereslett.springeropen.com

<1 %

29

Rakhmawati FARMA, Mohamad DERAMAN, Sepideh SOLTANINEJAD, AWITDRUS et al. "A New Approach towards Improving the Specific Energy and Specific Power of a Carbon-Based Supercapacitor using Platinum-Nanoparticles on Etched Stainless Steel Current Collector", Electrochemistry, 2015

Publication

<1 %

30

Ralf Th. Krampe, Ralf Engbert, Reinhold Kliegl. "Age-specific problems in rhythmic timing.", Psychology and Aging, 2001

Publication

<1 %

31

aip.scitation.org

Internet Source

<1 %

32

Chitrakshi Goel, Haripada Bhunia, Pramod K. Bajpai. " Resorcinol–formaldehyde based nanostructured carbons for CO adsorption: kinetics, isotherm and thermodynamic studies ", RSC Advances, 2015

Publication

<1 %

33

W B Kurniawan, A Indriawati, D Marina. " The Effect of Particle Size on the Performance of Electrode Supercapacitor based on Pepper () Shell Activated Carbon ", IOP Conference Series: Earth and Environmental Science, 2019

<1 %

34

G.D. Webler, W.C. Rodrigues, A.E.S. Silva, A.O.S. Silva et al. "Use of micrometric latex beads to improve the porosity of hydroxyapatite obtained by chemical coprecipitation method", *Applied Surface Science*, 2018

Publication

<1 %

35

Awitdrus, R Juliani, E Taer, R Farma, Iwantono, M Deraman. "Supercapacitor Electrodes Based on Corn Stalk Binderless Activated Carbon", *Journal of Physics: Conference Series*, 2018

Publication

<1 %

36

www.tandfonline.com

Internet Source

<1 %

37

Erman Taer, Mohamad Deraman, Ibrahim Abu Talib, Akrajas Ali Umar, Munetaka Oyama, Rozan Mohamad Yunus. "Physical, electrochemical and supercapacitive properties of activated carbon pellets from pre-carbonized rubber wood sawdust by CO₂ activation", *Current Applied Physics*, 2010

Publication

<1 %

38

R. Taslim, T.R. Dewi, E. Taer, A. Apriwandi, A. Agustino, R. N. Setiadi. "Effect of physical activation time on the preparation of carbon electrodes from pineapple crown waste for supercapacitor application", *Journal of Physics:*

<1 %

39

Goutam Chattopadhyaya, Douglas G. Macdonald, Narendra N. Bakhshi, Jafar S. Soltan Mohammadzadeh, Ajay K. Dalai. "Preparation and characterization of chars and activated carbons from Saskatchewan lignite", Fuel Processing Technology, 2006

Publication

<1 %

40

E Taer, P Kurniawan, R Taslim, A Agustino, Apriwandi, A Afrianda. "Carbon electrode based on durian shell: effects concentration of chemical activator agent (Potassium hydroxide)", Journal of Physics: Conference Series, 2018

Publication

<1 %

41

Naqing Mao, Lijin Huang, Qin Shuai. "Facile Synthesis of Porous Carbon for the Removal of Diclofenac Sodium from Water", ACS Omega, 2019

Publication

<1 %

42

Kabir O. Oyedotun, Farshad Barzegar, Abdulmajid A. Mirghni, Abubakar A. Khaleed, Tshifhiwa M. Masikhwa, Ncholu Manyala. "Examination of High-Porosity Activated Carbon Obtained from Dehydration of White Sugar for Electrochemical Capacitor Applications", ACS

<1 %

43

Jinhui Cao, Chunyu Zhu, Yoshitaka Aoki, Hiroki Habazaki. "Starch-Derived Hierarchical Porous Carbon with Controlled Porosity for High Performance Supercapacitors", ACS Sustainable Chemistry & Engineering, 2018

Publication

<1 %

44

Liang Chang, Kai Sun, Yun Hang Hu. "New Chemistry for New Material: Highly Dense Mesoporous Carbon Electrode for Supercapacitors with High Areal Capacitance", ACS Applied Materials & Interfaces, 2018

Publication

<1 %

45

Christoff Reimer, Michael R. Snowdon, Singaravelu Vivekanandhan, Xiangyou You et al. "Synthesis and characterization of novel nitrogen doped biocarbons from distillers dried grains with solubles (DDGS) for supercapacitor applications", Bioresource Technology Reports, 2019

Publication

<1 %